Biodegradation (2011) 22:13–23
DOI 10.1007/s10532-010-9370-z

ORIGINAL PAPER

Multisubstrate kinetics of PAH mixture biodegradation: analysis in the double-logarithmic plot

Mikhail Baboshin · Ludmila Golovleva

Received: 2 February 2010 / Accepted: 4 May 2010 / Published online: 20 May 2010
© Springer Science+Business Media B.V. 2010

Abstract The proposed method of kinetic analysis of aqueous-phase biodegradation of polycyclic aromatic hydrocarbons (PAH) mixture presupposes representation of kinetic curves for each pair of mixture components, S_x and S_y, in double-logarithmic coordinates (ln S_x; ln S_y). If PAH mixture conversion corresponds to the multisubstrate model with a common active site, then the graphs in double-logarithmic coordinates are straight lines with the angular coefficients equal to the ratio of respective first-order rate constants $k_x^y = \frac{V_y K_x}{K_y V_x}$, where K_x and K_y are half-saturation constants, V_x and V_y are the maximum conversion rates for substrates S_x and S_y; the graph slope does not depend on any concentrations and remains constant during the change of reaction rates as a result of inhibition, induction/inactivation of enzymes or biomass growth. The formulated method has been used to analyze PAH mixture conversion by the culture of *Sphingomonas* sp. VKM B-2434. It has been shown that this process does not satisfy the multisubstrate model with a single active site. The results suggest that the strain VKM B-2434 contains at least two dioxygenases of different substrate specificity: one enzyme converts phenanthrene and fluoranthene and the other converts acenaphthene and acenaphthylene. The ratios of first-order rate constants have been obtained for these pairs of substrates.

Keywords Multisubstrate kinetics · PAHs · *Sphingomonas* sp. VKM B-2434

M. Baboshin (✉) · L. Golovleva
G.K. Skryabin Institute of Biochemistry and Physiology of Microorganisms RAS, Prospekt Nauki 5, Pushchino, Moscow region, Russia
e-mail: mbaboshin@rambler.ru

Introduction

Polycyclic aromatic hydrocarbons (PAHs) are dangerous environmental pollutants; hence, PAH biodegradation is being intensively studied (Seo et al. 2009). In the environment, PAHs usually exist not as individual compounds but as components of complex mixtures, as in the case of soil pollution with oil or coal tar.

PAH biodegradation by microbial culture is liable to positive and negative effects of substrates and their conversion products. PAH conversion is retarded by substrate inhibition (Stringfellow and Aitken 1995) and inhibition by products (Casellas et al. 1998; Kazunga and Aitken 2000) and hastened by cross induction (Molina et al. 1999), co-metabolism (Bouchez et al. 1995), and the increase of biomass concentration during the growth (Guha et al. 1999). It is essential that the conversion rates of PAHs as mixture components differ from the conversion rates of individual PAHs due to metabolic interference of mixture components.

The study of the kinetics of PAH mixture bioconversion is important for understanding the mechanism of this process and for prediction of the rate of bioremediation of polluted environments. In most cases, aqueous-phase PAH mixture conversion can be satisfactorily described by a multisubstrate model, according to which all mixture components compete for the same common active site in accordance with the principles of Michaelis kinetics (Stringfellow and Aitken 1995; Guha et al. 1999; Lotfabad and Gray 2002; Knightes and Peters 2006; Dimitriou-Christidis and Autenrieth 2007; Desai et al. 2008).

This paper describes the method of analysis of the kinetic curves of PAH mixture conversion, which proves the correspondence of process under study with the above multisubstrate model and estimates the relative values of first-order rate constants for all mixture components.

Materials and methods

Reagents

Acenaphthylene (ACNL), acenaphthene (ACNT), phenanthrene (PHE), anthracene (ANT), fluoranthene (FLA), pyrene (PYR), naphthalene, dibenzofuran, and 1,5-, 1,8-, 2,3-, 2,6-, and 2,7-dimethylnaphthalenes were used as substrates and inhibitors; some of their structural formulas are shown in Fig. 1. Fluorene was used as internal standard. Hydrocarbons were of high purity grade (>98%; purchased from Sigma-Aldrich, Fluka, and Merck). Other reagents were produced in Russia (no less than analytical reagent grade). Ethyl acetate was distilled before use.

Substrate solutions

Substrate solutions were obtained by dissolving ACNL and ACNT in methanol in a concentration ~300 μmol/l for each compound; PHE, ANT, FLA and PYR in a concentration ~55 μmol/l for each compound. In some experiments, other polyaromatic compounds were added to substrate solutions or some components were excluded from substrate composition.

Incubation medium

The mineral medium contained (g/l): NH_4NO_3, 1.0; KH_2PO_4, 1.0; K_2HPO_4, 1.0; $MgSO_4 \cdot 7H_2O$, 0.2; $CaCl_2$, 0.02; $FeCl_3$, two drops of saturated solution, pH ~ 7.5. The mineral medium was filtered and sterilized. Vitamin B_{12} (1 μg/l) was added to the medium after sterilization. Eight hours prior to the experiment, the incubation medium was poured by 49 ml into flasks (50 ml), substrate solution was added by 200 μl, the flasks were tightly closed with glass caps and incubated for thermostating at 30°C with slow stirring from time to time. Initial concentrations in the incubation medium were ~1.2 μmol/l for ACNL and ACNT and ~0.22 μmol/l for other substrates, which was much less than the water solubility of all hydrocarbons used (Juhasz and Naidu 2000; Wammer and Peters 2005).

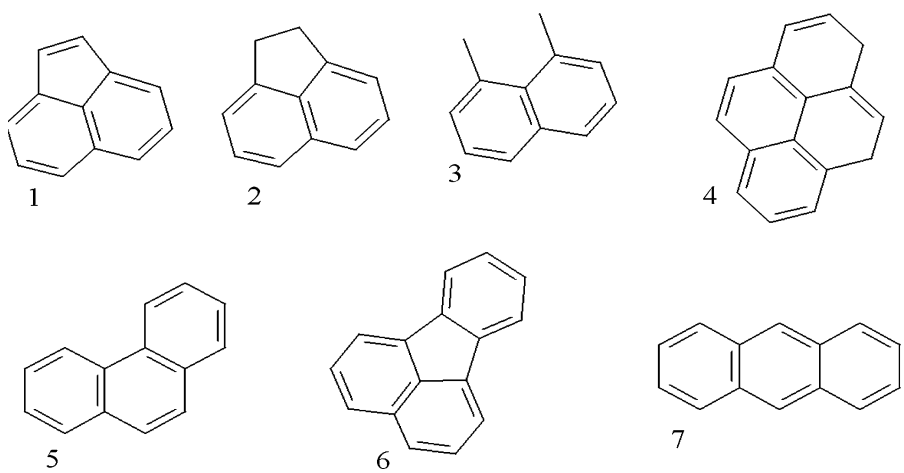

Fig. 1 Substances used as substrates and inhibitors: *1* acenaphthylene (ACNL); *2* acenaphthene (ACNT); *3* 1,8-dimethylnaphthalene (1,8DMN); *4* pyrene (PYR); *5* phenanthrene (PHE); *6* fluoranthene (FLA); *7* anthracene (ANT)

Microbial culture

The strain *Sphingomonas* sp. VKM B-2434 capable of PAH conversion has been characterized previously (Baboshin et al. 2008). Fed-batch microbial culture was obtained as follows: 1 ml of *Sphingomonas* sp. VKM B-2434 culture grown in the medium with ACNT (0.5 g/l) was added into a flask with 400 ml of the incubation medium and incubated at 30°C under stirring and bubbling by humid air saturated with ACNT vapor; for this purpose, the air (~1 l/min) was passed first through a bottle with water and then through a column (23 cm, Ø 12 mm) with crystalline ACNT and fed to the flask with the culture; the rate of ACNT feeding was ~12 μg/min. The culture demonstrated substrate-limited growth; linear increase of biomass concentration and negligible ACNT concentration were observed in the culture. After 96 h of incubation, the culture turbidity reached 0.38–0.40 OD values and the fed-batch culture was used in the experiments. The same culture killed by boiling (5 min) was used in sterile control experiments.

Experimental procedure

Microbial culture (1 ml) was added into a flask with the incubation medium; the flask was tightly closed with a glass cap and incubated on a shaker at 30°C for a certain period of time (1–40 min). Incubation was stopped by adding 0.5 ml of 5 N sulfuric acid solution.

Sample processing

After the incubation, 20 μg of fluorene in 1 ml of ethyl acetate (internal standard) and 5 N potassium hydroxide solutions (0.5 ml) were introduced into the flask. The liquid was twice extracted with ethyl acetate, (20 + 10) ml. The extracts were evaporated in a rotor evaporator at 38°C under vacuum (~100 mbar), with preliminary addition of 100 μl of dimethylformamide into each extract. Ethyl acetate vaporized and dimethylformamide remained. Thus, extracted hydrocarbons (including the internal standard) were dissolved in a small volume of dimethylformamide in the concentrations sufficient for gas chromatography.

Gas chromatography of the extracts

Hydrocarbon concentrations in the extracts were determined by gas chromatography in a Kristall-2000 M chromatograph (Chromatec, Russia) with a flame-ionizing detector and a HP-5 column (30 m × 0.32 mm × 0.25 μm). The evaporator and detector temperatures were 250 and 290°C, respectively. The column temperature increased from 160 to 260°C during the analysis at a rate of 10°C/min. Hydrocarbon mass in a sample (μg) was calculated by the ratio of the hydrocarbon peak area to the peak area of internal standard (fluorene):

$$m_i = \frac{\beta_{FLU}}{\beta_i}\frac{A_i}{A_{FLU}} * 20, \tag{1}$$

where $\frac{\beta_{FLU}}{\beta_i}$ was the ratio of fluorene and the hydrocarbon analytic sensitivities; $\frac{A_i}{A_{FLU}}$ was the ratio of the hydrocarbon and fluorene peak areas; and 20 was fluorene mass in a sample (μg).

Theory

In accordance with the multisubstrate model with a common active site (further referred to as MCAS-model), n substrates (S_1, S_2,…,S_n) compete for a single active site E according to the scheme

$$\begin{gathered} S_1 + E \underset{[k_1^{(1)}]}{\longrightarrow} ES_1, S_2 + E \underset{[k_1^{(2)}]}{\longrightarrow} ES_2, \ldots, S_n + E \underset{[k_1^{(n)}]}{\longrightarrow} ES_n, \\ ES_1 \underset{[k_{-1}^{(1)}]}{\longrightarrow} E + S_1, ES_2 \underset{[k_{-1}^{(2)}]}{\longrightarrow} E + S_2, \ldots, ES_n \underset{[k_{-1}^{(n)}]}{\longrightarrow} E + S_n, \\ ES_1 \underset{[k_2^{(1)}]}{\longrightarrow} E + P_1, ES_2 \underset{[k_2^{(2)}]}{\longrightarrow} E + P_2, \ldots, ES_n \underset{[k_2^{(n)}]}{\longrightarrow} E + P_n. \end{gathered} \tag{2}$$

Applying quasi-steady-state approximation to the scheme (2), one can derive the following formula for the rate of conversion of any substrate S_i (Segel 1975; Guha et al. 1999; Desai et al. 2008):

$$v_i = \frac{V_i S_i}{K_i + \sum_{j=1}^{n} \frac{K_i}{K_j} S_j}, \tag{3}$$

where $V_i = k_2^{(i)} E$ is the maximum rate of reaction i (i.e., the rate of complete saturation of the active site with substrate S_i) and $K_j = \frac{k_{-1}^{(j)} + k_2^{(j)}}{k_1^{(j)}}$ is Michaelis constant for substrate S_j.

Formula (3) has an interesting property, which as yet has escaped researchers' attention and has not been used in any way. It turns out that the ratio of conversion rates for any pair of substrates S_x and S_y from the series (S_1, S_2,…,S_n) is proportional to the ratio of their concentrations:

$$\frac{v_y}{v_x} = k_x^y \frac{S_y}{S_x}, \tag{4}$$

where

$$k_x^y = \frac{V_y K_x}{K_y V_x} \tag{4a}$$

is the ratio of first-order rate constants for substrates S_x and S_y (in other words, the ratio of their specific affinity constants).

Indeed, if the system contains two substrates ($n = 2$), their conversion rates, according to formula (3), are determined by expressions

$$v_1 = \frac{V_1 S_1 K_2}{K_1 K_2 + S_1 K_2 + K_1 S_2} \text{ and}$$
$$v_2 = \frac{K_1 V_2 S_2}{K_1 K_2 + S_1 K_2 + K_1 S_2},$$

and their ratio

$$\frac{v_1}{v_2} = \frac{V_1 K_2}{K_1 V_2} \frac{S_1}{S_2} = k_2^1 \frac{S_1}{S_2}$$

corresponds to formula (4). In the presence of three substrates in the system ($n = 3$), their conversion rates are determined by expressions

$$v_1 = \frac{V_1 S_1 K_2 K_3}{K_1 K_2 K_3 + S_1 K_2 K_3 + K_1 S_2 K_3 + K_1 K_2 S_3},$$
$$v_2 = \frac{K_1 V_2 S_2 K_3}{K_1 K_2 K_3 + S_1 K_2 K_3 + K_1 S_2 K_3 + K_1 K_2 S_3}, \text{ and}$$
$$v_3 = \frac{K_1 K_2 V_3 S_3}{K_1 K_2 K_3 + S_1 K_2 K_3 + K_1 S_2 K_3 + K_1 K_2 S_3},$$

and the ratios of the rates as well satisfy the property (4):

$$\frac{v_1}{v_2} = \frac{V_1 K_2}{K_1 V_2} \frac{S_1}{S_2} = k_2^1 \frac{S_1}{S_2}; \quad \frac{v_2}{v_3} = \frac{V_2 K_3}{K_2 V_3} \frac{S_2}{S_3} = k_3^2 \frac{S_2}{S_3};$$
$$\frac{v_1}{v_3} = \frac{V_1 K_3}{K_1 V_3} \frac{S_1}{S_2} = k_3^1 \frac{S_1}{S_3}.$$

With an arbitrary quantity of substrates in the system (any n), the their conversion rates are also expressed in fractions, where denominators are identical and the ratio of numerators results in formula (4), because the half-saturation constants of all other substrates, except for the pair under consideration, are reciprocally cancelled. Integration of Eq. 4 leads to:

$$\ln S_y = k_x^y \ln S_x + \left(\ln S_y^0 - k_x^y \ln S_x^0\right). \tag{5}$$

Consequently, if substrate conversion satisfies the MCAS-model, then the graph in double-logarithmic coordinates (ln S_x; ln S_y) is a line segment with the angular coefficient equal to the ratio of respective first-order rate constants. The angular coefficient of graph (5) does not depend on any concentrations and remains constant on the addition of inhibitors of conversion of tested substrates and on the change of catalytic activity as a result of growth or induction/inactivation of biomass. Indeed, during the inhibition of conversion of substrates S_x and S_y in the common active site, the kinetic parameters V_x and V_y, K_x and K_y change in proportion to each other and, according to formula (4a), the angular coefficient k_x^y remains unchanged; the change of concentration of the active site itself will result in proportional alteration of parameters V_x and V_y at constant K_x and K_y, and coefficient k_x^y will also remain constant.

Thus, the constancy of graph slope in double-logarithmic coordinates under different changes of concentrations in the studied system is a criterion of correspondence with the MCAS-model, and the angular coefficients of these graphs make allow estimation of the relative values of first-order rate constants for conversion of each substrate. This approach has been used for the analysis of PAH conversion by the strain *Sphingomonas* sp. VKM B-2434.

Results

The analysis of aqueous-phase PAH mixture conversion by the strain *Sphingomonas* sp. VKM B-2434

Conversion of the mixture of four substrates (PHE, ANT, FLA, and PYR) has been studied with ACNL, ACNT, dibenzofuran, naphthalene, and five isomeric dimethylnaphthalenes used as inhibitors. All of these substances significantly retarded substrate conversion; the maximum change of graph slopes in double-

logarithmic coordinates was observed in the presence of naphthalene 1,8-derivatives: ACNL, ACNT, and 1,8-dimethylnaphthalene (1,8DMN). Results of the two most informative experiments are given below. No changes of PAH concentrations were observed in sterile control experiments.

In the presence of ACNL and ACNT in the medium, the rates of conversion of each of the above four substrates significantly decreased (Fig. 2). The graphs in double-logarithmic coordinates (Fig. 3) can be considered as linear for most of the substrate pairs; however, graph slopes in the presence and absence of inhibitors are highly different in all cases but one: for the PHE–FLA pair, the angular coefficient was unchanged during the inhibition (Fig. 3b). These data lead to the following conclusions: (1) conversion of the pairs of substrates PHE–ANT, PHE–PYR, ANT–FLA, and ANT–PYR do not satisfy the MCAS-model; (2) the substrates form a series of $ANT < PHE = FLA < PYR$ by sensitivity to inhibition, i.e., PYR conversion is inhibited maximally and ANT conversion is inhibited minimally, while PHE and FLA conversions are inhibited equally, with an intermediate value of inhibition (as follows from comparison of the angular coefficients of the graphs in the presence and absence of inhibition); and (3) conversion of the PHE-FLA pair seems to correspond to the MCAS-model, with the catalytic activity being 3.6 times higher for FLA than for PHE: $k_{PHE}^{FLA} = 3.6$. With other inhibitors, the angular coefficient of the graph also acquired values close to 3.6.

Further, conversion of a mixture of six substrates (ACNL, ACNT, PHE, ANT, FLA, and PYR) was compared in the absence of other hydrocarbons and in the presence of 1,8DMN as an inhibitor. 1,8DMN substantially reduced the rate of ACNL and ACNT conversion but had no effect on conversion of other four substrates (Fig. 4). The graphs in double-logarithmic coordinates for the ACNL–ACNT pair are linear, with the same angular coefficient with and without the inhibitor, while for ACNL–PHE, ACNL–ANT, and ACNL–FLA they are curves and do not coincide during incubation in the presence and absence of the inhibitor (Fig. 5). The graphs for ACNL–PYR cannot be satisfactorily smoothed by the lines due to the very low rate of PYR conversion

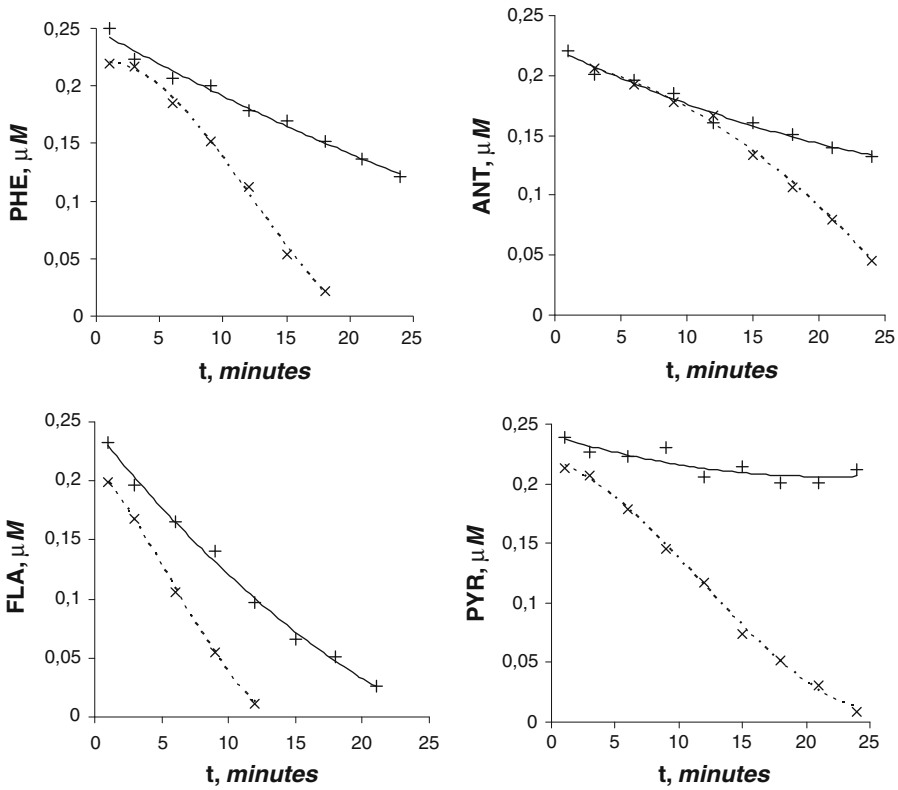

Fig. 2 Conversion curves of ACNL, ACNT, PHE, ANT, FLA, and PYR in a mixture in the absence of other hydrocarbons (*cross*) and in the presence of ACNL and ACNT, both in the initial concentration of 1.15 μmol/l, (*plus*)

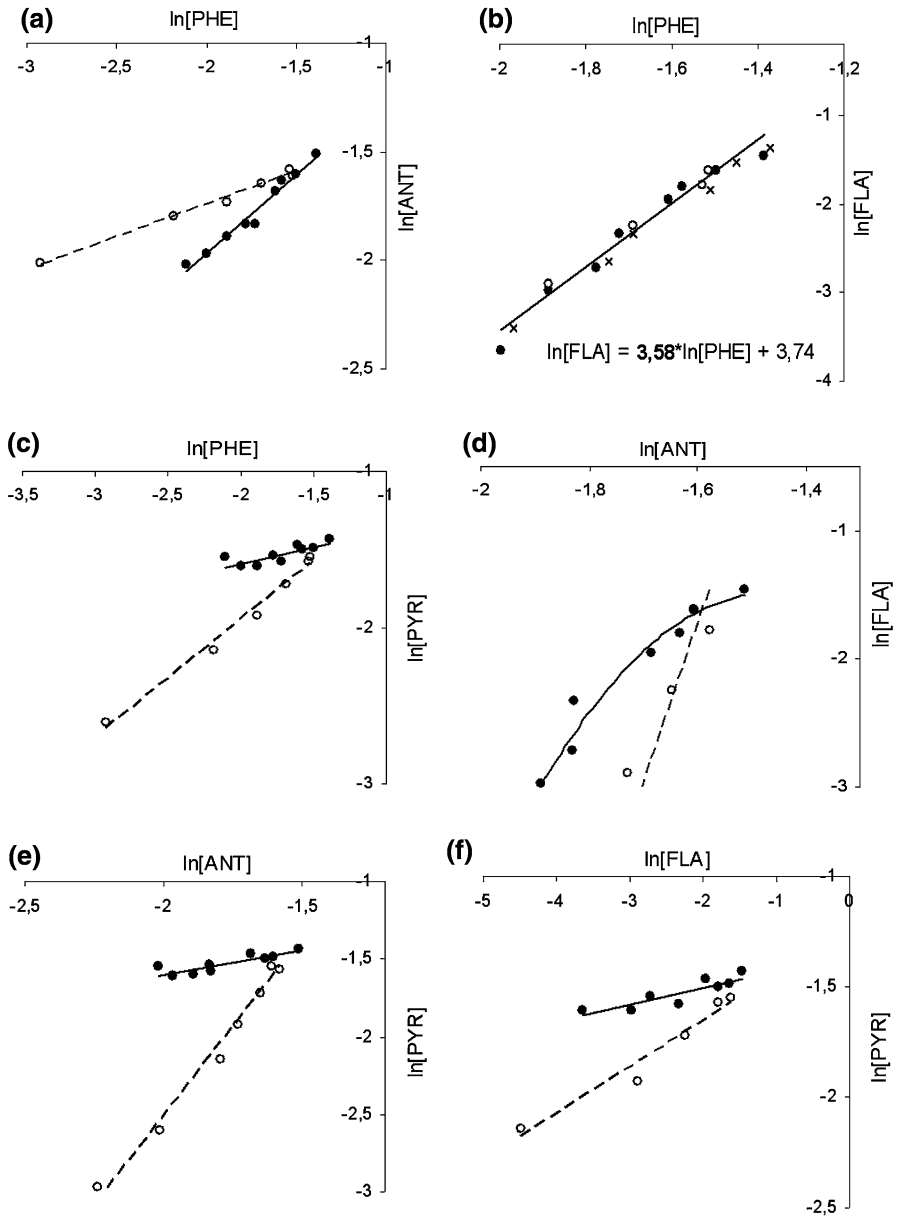

Fig. 3 Double-logarithmic plot for PHE, ANT, FLA, and PYR conversion in a mixture in the absence of other hydrocarbons (*open circle*) and in the presence of ACNL and ACNT (*filled circle*). Figure **b** shows the data on conversion of the PHE–FLA pair in the subsequent experiment (*cross*)

under the given conditions (Fig. 5e). Thus, the conversion of ACNL and ACNT seems to correspond to the multisubstrate kinetics with the common active site, different from the previously postulated active site for PHE–FLA. Catalytic activity is 3.3 times higher for ACNL than for ACNT: $k_{ACNL}^{ACNT} = 0.30 \approx 1/3.3$. The conversion of ANT together with the ACNL–ACNT pair does not satisfy the MCAS-model. It is not clear from the data obtained whether PYR reacts in the same active site as ACNL–ACNT.

Discussion

In contrast to most of the previous studies of the kinetics of PAH mixture conversion (Guha et al. 1999; Knightes and Peters 2006; Dimitriou-Christidis and Autenrieth 2007; Desai et al. 2008), in this work we have concentrated our attention on the direct analysis of the curves of PAH mixture conversion without resorting to sole-substrate experiments. We have shown theoretically that in the case of multisubstrate

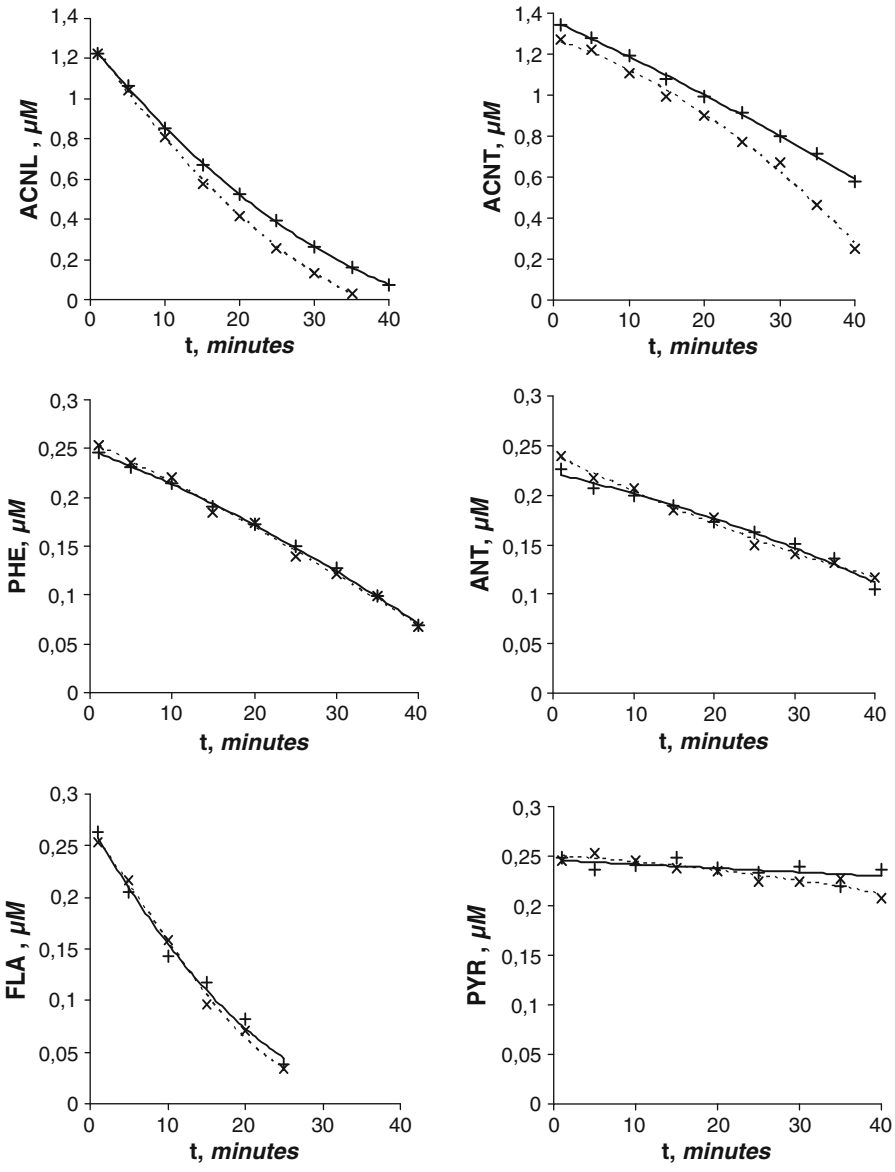

Fig. 4 Conversion curves of ACNL, ACNT, PHE, ANT, FLA, and PYR in a mixture in the absence of other hydrocarbons (*cross*) and in the presence of 1,8DMN in the initial concentration of 2.6 μmol/l (*plus*)

kinetics with a common active site the logarithms of substrate concentrations are linearly dependent. It means that conversion of an arbitrarily complex mixture of substrates can be described by a single function. Indeed, it follows from Eq. 5 that the kinetic curves represented in the coordinates $\left(t; \ln\frac{S_0}{S}\right)$ can be superposed by compression to the axis of time with compression factors proportional to the first-order rate constants for each substrate.

Besides testing the conformance of PAH mixture to the MCAS-model, our method makes it possible to estimate the relative values of first-order rate constants for each component of the mixture. These constants characterize biodegradability of the substrates (Wammer and Peters 2005) and define the relative values of PAH conversion at low concentrations in the aqueous phase ($S_i \ll K_i$), which takes place under limited bioavailability of PAH (Lotfabad and Gray 2002). Coefficients k_x^y can also be used for adjustment of the values of kinetic parameters obtained from sole-substrate experiments.

In this work, as in the earlier studies of other authors, the kinetics of PAH mixture conversion has been described using an MCAS-model presupposing

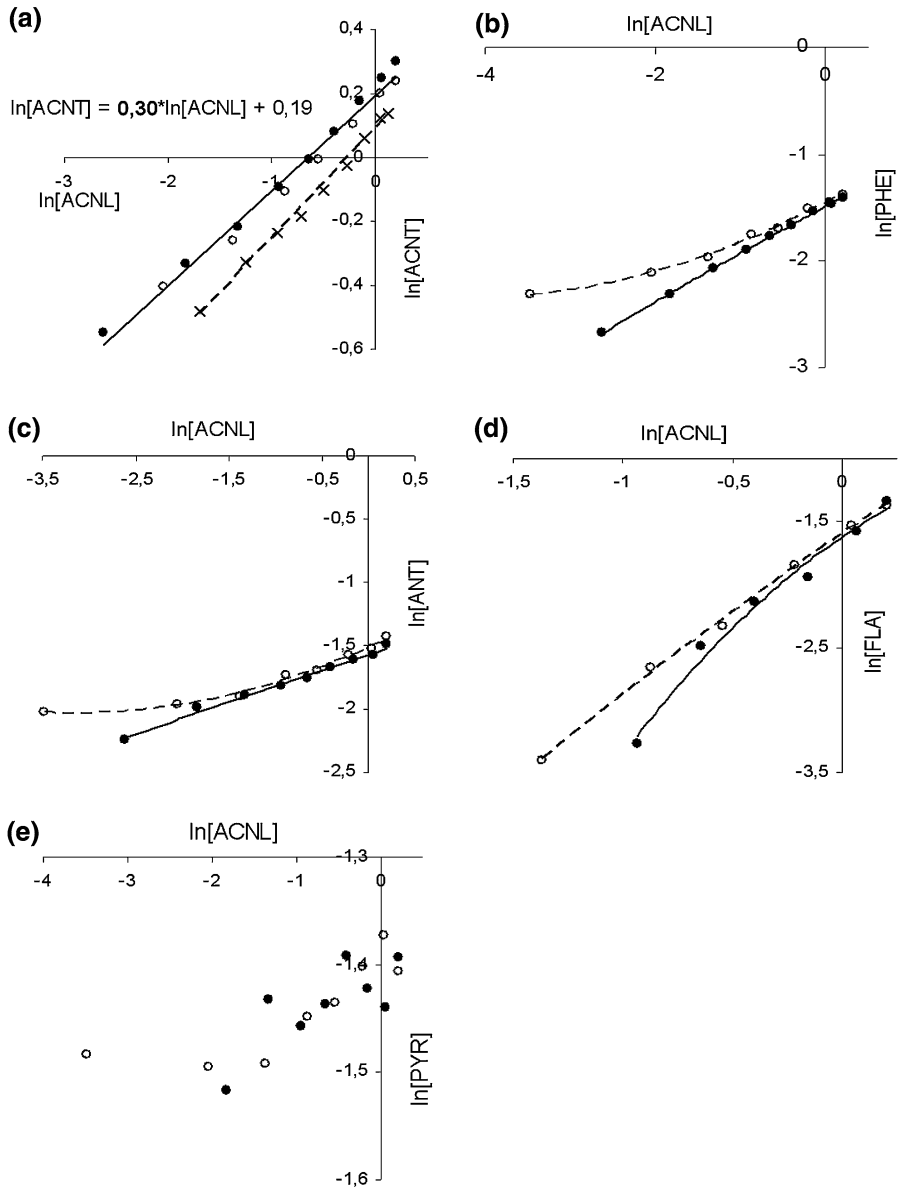

Fig. 5 Double-logarithmic plot for ACNL, ACNT, PHE, ANT, FLA, and PYR conversion in a mixture in the absence of other hydrocarbons (*open circle*) and in the presence of 1,8DMN (*filled circle*). Figure **a** shows the data on conversion of the ACNL–ACNT pair in the preceding experiment (*cross*)

the competition of several substrates for a single active site. The processes in microbial cultures are much more complex than this model. Deviation of the rate of conversion from the value predicted by the formula (3) may be caused by: (1) biomass growth or induction of enzyme systems during the experiment; (2) sorption of substrates by the biomass and the surface of fermenter and the presence of substrates as a solid phase; and (3) existence of several alternative systems of substrate conversion. Let us consider the above factors in more detail.

Experiments on PAH mixture conversion are usually performed in microbial cultures with pre-induced enzyme systems of PAH conversion; otherwise, the kinetic curves with a lag phase are observed, which do not satisfy the MCAS-model (Lotfabad and Gray 2002). Biomass growth is either taken into account in the course of modeling (Guha et al. 1999; Knightes and Peters 2006), or the experiments are performed under so-called extant conditions (Grady et al. 1996) when growth can be neglected (Dimitriou-Christidis and Autenrieth 2007;

Desai et al. 2008; present paper). For analysis in the double-logarithmic plot, the induction and growth are indifferent: as is shown in the "Theory" section, the graph slope remains constant during the change of active site concentration. Thus, the double-logarithmic plot is applicable in unsteady state by catalytic activity (for instance, to initially uninduced cultures) and does not require any correction for biomass growth.

The second factor, i.e., sequestration of substrates into non-aqueous phases, results in substantial deviations from the MCAS-model in the systems with hydrophobic surfaces, non-aqueous-phase liquids, or solid PAHs. Effective (aqueous) substrate concentrations ($S_i^{(aq)}$) in such systems are less than the measured values (S_i). In the presence of substantial sequestration of substrates into non-aqueous phases, this phenomenon is taken into account in the model (Guha et al. 1999; Lotfabad and Gray 2002). In our experiments, as in most of the works on this subject, PAH concentrations were lower than their aqueous solubility and the solid phase was absent. The principal factor of sequestration of substrates seemed to be their sorption by the biomass. Being hydrophobic substances, PAHs can be solved in biomembranes, and the coefficient of sorption correlates with the substance hydrophobicity, i.e., with the octanol–water partition coefficient (Baughman and Paris 1981). Among the PAHs we used, fluoranthene and pyrene were the most hydrophobic. Bacterial sorption coefficient of pyrene as estimated earlier (*ibid.*) is equal to $K_{PYR}^{(sorb)} = 2.7 * 10^4$. Biomass concentration in our experiments was approximately $B = 5$ ppm. Consequently, the amount of sorbed pyrene was about seven times less compared to that solved in the water phase: $K_{PYR}^{(sorb)} * B = 0.135 \approx 1/7$. Thus, the sorption of even the most hydrophobic substrates of those used was rather low at such a low biomass concentration. It is more interesting that even substantial sorption of substrates, significantly retarding their conversion, has no effect on the double-logarithmic plot. If the sorption of substrates S_x and S_y can be described by partition coefficients

$$K_x^{(sorb)} = \frac{S_x - S_x^{(aq)}}{S_x^{(aq)}}, \quad K_y^{(sorb)} = \frac{S_y - S_y^{(aq)}}{S_y^{(aq)}}, \qquad (6)$$

and the conditions of MCAS-model are satisfied for the aqueous concentrations

$$\ln S_y^{(aq)} = k_x^y \ln S_x^{(aq)} + \left(\ln S_y^{0(aq)} - k_x^y \ln S_x^{0(aq)}\right), \qquad (7)$$

then the double-logarithmic plot for total concentrations (S_x and S_y) will also be a straight line with angular coefficient k_x^y, because Eq. 5 follows from the system of Eqs. 6 and 7. It means that the method of double-logarithmic plot is not confined to the aqueous-phase kinetics but also applicable in the presence of sorption equilibria in the system. Under significant diffusion limitations, when the sorption/desorption process is far from equilibrium, Eq. 6 are not satisfied and the double-logarithmic plot will be distorted. However, existence of such diffusion limitations in bacterial cell suspensions seems to be unlikely.

The third cause of possible deviations for the model with a single active site consists in the complex organization of a real metabolic system compared to the model. The formulated approach permits certain assumptions as regards the quantity of active PAH conversion sites in the microbial culture under study. Obviously, the conversion of substrates satisfies the MCAS-model, if their metabolic pathways have a common flux-generating step (Crabtree and Newsholme 1987), i.e., the sequence of reactions prior to the first irreversible reaction, including the latter. PAH utilization by bacteria begins with an irreversible dioxygenase reaction; therefore, in the absence of diffusion limitations, the unchanged graph slope in double-logarithmic coordinates can be interpreted as the presence of a common first enzyme in the PAH metabolic pathways, while the change of inclination of the graph may be evidence that the metabolic pathways of given substrates begin on different enzymes. Thus, the results suggest that PAH conversion by the culture of *Sphingomonas* sp. VKM B-2434 begins on different enzymes. It seems that there is a common active site for the ACNL–ACNT pair and another active site for the PHE-FLA pair. It is significant that the substrates from each of these pairs have higher structural similarity between them than to other substrates (Fig. 1). It is in agreement with conclusions from the study (Wammer and Peters 2006) showing that the rate of hydrocarbon oxidation by naphthalene oxygenase is determined mainly by the structure but not thermodynamic characteristics of a substrate.

According to the literature data, different bacterial strains may have the common or different enzymes

catalyzing PAH oxidation. The conversion of naphthalene, 1,5-dimethylnaphthalene, and fluorene by the strain *Sphingomonas* sp. EPA 505 satisfies the MCAS-model (Desai et al. 2008). In the strain *Sphingomonas* sp. CHY-1, the presence of a single enzyme for oxidation of polyaromatic hydrocarbons has been shown by introduction of a mutation into the respective gene (Demaneche et al. 2004). On the other hand, in spite of prediction by the MCAS-model, the conversion of 1-methylfluorene by the strain EPA 505 was not affected by the presence of naphthalene and 1,5-dimethylnaphthalene (Desai et al. 2008). The strain *Mycobacterium vanbaalenii* PYR-1 possesses several copies of dioxygenase genes (Kim et al. 2006); two oxygenases found in the strain *Mycobacterium* sp. 6PY1 differ in substrate specificities to phenanthrene and pyrene (Krivobok et al. 2003). The results of our kinetic experiments do not satisfy the MCAS-model and are evidence of the probable presence of at least two dioxygenases of different substrate specificity in *Sphingomonas* sp. VKM B-2434. It should be noted that the unconformity of conversion of two substrates to the MCAS-model does not imply the absence of the common site of their conversion. A situation is possible, e.g., when there is one more site (besides the common active site) specific to one of the substrates; hence, the question about the quantity of active sites needs further investigation.

The question whether two enzymatic reactions take place in the same active site or in different sites was solved previously by the method of competition plot (Chevillard et al. 1993). This method was further used in several tens of enzymological studies; but it seems to be inapplicable for the study of microbial cultures as it presupposes the measurement of initial steady-state reaction rates. The method of double-logarithmic plot described in the present work has the following advantages as compared with the previous method (Chevillard et al. 1993): (1) it is quantitative, i.e., provides for estimation of the ratios of first-order rate constants for reactions with the common active site; (2) it is applicable in unsteady state by catalytic activity; this is important, because enzyme induction/inactivation and microbial growth during the measurement is usually an obstacle for correct assessment of the kinetic parameters of microbial cultures (Grady et al. 1996); and (3) it presupposes the measurement of not reaction rates but the ratios of substrate concentrations, making much lesser demands on the accuracy of chemical and analytical methods.

References

Baboshin MA, Akimov VN, Baskunov BP, Born TL, Khan SU, Golovleva LA (2008) Conversion of polycyclic aromatic hydrocarbons by *Sphingomonas* sp. VKM B-2434. Biodegradation 19:567–576

Baughman G, Paris DF (1981) Microbial bioconcentrations of organic pollutants from aquatic systems—a critical review. CRC Crit Rev Microbiol 8:205–228

Bouchez M, Blanchet D, Vandecasteele JP (1995) Degradation of polycyclic aromatic hydrocarbons by pure strains and defined strain associations: inhibition phenomena and cometabolism. Appl Microbiol Biotechnol 43:156–164

Casellas M, Grifoll M, Sebate J, Solanas AM (1998) Isolation and characterization of a fluorenone-degrading bacterial strain and its role in synergistic degradation of fluorene by a consortium. Can J Microbiol 44:734–742

Chevillard C, Cardenas ML, Cornish-Bowden A (1993) The competition plot: a simple test of whether two reactions occur at the same active site. Biochem J 289:599–604

Crabtree B, Newsholme EA (1987) A systematic approach to describing and analyzing metabolic control systems. Trends Biochem Sci 12:4–12

Demaneche S, Meyer C, Micoud J, Louwagie M, Willison JC, Jouanneau Y (2004) Identification and functional analysis of two aromatic-ring-hydroxylating dioxygenases from a *Sphingomonas* strain that degrades various polycyclic aromatic hydrocarbons. Appl Environ Microbiol 70:6714–6725

Desai AM, Autenrieth RL, Dimitriou-Christidis P, McDonald TJ (2008) Biodegradation kinetics of select polycyclic aromatic hydrocarbon (PAH) mixtures by *Sphingomonas paucimobilis* EPA505. Biodegradation 19:223–233

Dimitriou-Christidis P, Autenrieth RL (2007) Kinetics of biodegradation of binary and ternary mixtures of PAHs. Biotech Bioeng 97:788–800

Grady CPL Jr, Smets BF, Barbeau DS (1996) Variability in kinetic parameter estimates: a review of possible causes and a proposed terminology. Water Res 30:742–748

Guha S, Peters CA, Jaffé PR (1999) Multisubstrate biodegradation kinetics of naphthalene, phenanthrene, and pyrene mixtures. Biotech Bioeng 65:491–499

Juhasz AL, Naidu R (2000) Bioremediation of high molecular weight polycyclic aromatic hydrocarbons: a review of microbial degradation of benzo[*a*]pyrene. Int Biodeterior Biodegrad 45:57–88

Kazunga C, Aitken MD (2000) Products of incomplete metabolism of pyrene by polycyclic aromatic hydrocarbon-degrading bacteria. Appl Environ Microbiol 66:1917–1922

Kim S-J, Kweon O, Freeman JP, Jones RC, Adjei MD, Jhoo J-W, Edmondson RD, Cerniglia CE (2006) Molecular cloning and expression of genes encoding a novel dioxygenase involved in low- and high-molecular-weight polycyclic aromatic hydrocarbon degradation in *Mycobacterium vanbaalenii* PYR-1. Appl Environ Microbiol 72:1045–1054

Knightes CD, Peters CA (2006) Multisubstrate biodegradation kinetics for binary and complex mixtures of polycyclic aromatic hydrocarbons. Environ Toxicol Chem 25:1746–1756

Krivobok S, Kuony S, Meyer C, Louwagie M, Willison JC, Jouanneau Y (2003) Identification of pyrene-induced proteins in *Mycobacterium* sp. strain 6PY1: evidence for two ring-hydroxylating dioxygenases. J Bacteriol 185:3828–3841

Lotfabad SK, Gray MR (2002) Kinetics of biodegradation mixtures of polycyclic aromatic hydrocarbons. Appl Microbiol Biotechnol 60:361–366

Molina M, Araujo R, Hodson RE (1999) Cross-induction of pyrene and phenanthrene in a *Mycobacterium* sp. isolated from polycyclic aromatic hydrocarbon contaminated river sediments. Can J Microbiol 45:520–529

Segel IH (1975) Enzyme kinetics. Wiley, New York

Seo J-S, Keum Y-S, Li QX (2009) Bacterial degradation of aromatic compounds. Int J Environ Res Public Health 6:278–309

Stringfellow WT, Aitken MD (1995) Competitive metabolism of naphthalene, methylnaphthalene and fluorene by phenanthrene-degrading pseudomonads. Appl Environ Microbiol 61:357–362

Wammer KH, Peters CA (2005) Polycyclic aromatic hydrocarbon biodegradation rates: a structure-based study. Environ Sci Technol 39:2571–2578

Wammer KH, Peters CA (2006) A molecular modeling analysis of polycyclic aromatic hydrocarbon biodegradation by naphthalene dioxygenase. Environ Toxicol Chem 25:912–920